New nine-node Lagrangian quadrilateral plate element based on Mindlin-Reissner theory using IFM

H.R. Dhananjaya*[1,2], P.C. Pandey[3a], J. Nagabhushanam[4b] and Zainah Ibrahim[2c]

[1]*Department of Civil Engineering, Nitte Meenakshi Institute of Technology, Bangalore-560 064, India*
[2]*Department of Civil Engineering, University of Malaya, Kuala Lumpur-50603, Malaysia*
[3]*Department of Civil Engineering, Indian Institute of Science, Bangalore-560 012, India*
[4]*Department of Aerospace Engineering, Indian Institute of Science, Bangalore-560 012, India*

Abstract. This paper presents a new nine-node Lagrangian quadrilateral plate bending element (MQP9) using the Integrated Force Method (IFM) for the analysis of thin and moderately thick plate bending problems. Three degrees of freedom: transverse displacement w and two rotations θ_x and θ_y are considered at each node of the element. The Mindlin-Reissner theory has been employed in the formulation which accounts the effect of shear deformation. Many standard plate bending benchmark problems have been analyzed using the new element MQP9 for various grid sizes via Integrated Force Method to estimate defections and bending moments. These results of the new element MQP9 are compared with those of similar displacement-based plate bending elements available in the literature. The results are also compared with exact solutions. It is observed that the presented new element MQP9 is free from shear locking and produced, in general, excellent results in all plate bending benchmark problems considered.

Keywords: integrated force method; mindlin-reissner plate theory stress-resultant fields; displacement fields; shear locking

1. Introduction

 The finite element stiffness method, which is based on an assumed displacement field, has become the method of choice for solving a wide variety of problems in structural mechanics. The advantages of the stiffness method include (i) the capability to efficiently and accurately model domains with complex geometric configurations and varying material properties and (ii) the capability to accurately analyze problems with geometrical and material nonlinearities. The development of finite stiffness elements and their corresponding formulations has been a subject of extensive research.

 Shortcomings of the assumed displacement method have been observed in the analyses of certain classes of problems, such as modeling nearly incompressible materials, bending of thin plates, and optimizing structures. Moreover, since stresses are calculated indirectly by using displacement derivatives, the accuracy of stress predictions may be reduced. Two alternative finite element

---

*Corresponding author, Professor, E-mail: djaya_hr@yahoo.com; djaya_hr@um.edu.my
[a]Professor
[b]Emeritus Professor
[c]Senior Lecturer

formulations may be utilized to analyze the aforementioned problems and to calculate stress more accurately: (i) the hybrid stress method, and (ii) the force method. Because both of these formulations have certain disadvantages compared to the assumed displacement method, their use and availability in general purpose programs has been limited. In the hybrid method, the flexibility matrix must be inverted in order to generate the element stiffness matrix; this can become a computational burden, especially if high order approximations of stress fields are required. In the standard force method, on the other hand, an auxiliary statically determinate structure and a corresponding set of redundant forces must be selected. This process is not easily adapted to computer automation. Several attempts have been made to improve the process by which redundancies are selected. The pertinent formulations were summarized by Kaneko *et al.* (1983). All of these procedures, however, either resulted in matrices with certain undesired properties or lacked a physical interpretation, which made them unattractive to the engineering community and led to the demise of the standard force method.

An alternate formulation, termed the Integrated Force Method (IFM), has been developed by Patnaik (Patnaik 1973) to analyze problems in structural mechanics. It is a new formulation for computerizing the classical force method of analysis. In the Integrated Force Method all independent forces are treated as unknown quantities that can be calculated by simultaneously imposing both equilibrium and compatibility conditions. Generation of compatibility conditions for elasticity and discrete models have been reported by Patnaik *et al.* (2000). Nagabhushanam and Patnaik (1990) have developed a general purpose program to generate compatibility matrix for the IFM. Automatic generation of sparse and banded compatibility matrix for the Integrated Force Method has been reported by Nagabhushanam and Srinivas (1991). IFM has been successfully implemented for analyzing, plane stress problems (Nagabhushanam and Srinivas 1991), two/three dimensional problems (Kaljevic *et al.* 1996, Kaljevic *et al.* 1996), dynamics (Patnaik and Yadagiri 1976), Optimization (Patnaik *et al.* 1986) and non-linear problems (Krishnam Raju and Nagabhushanam 2000). A 4-node rectangular plate bending element based on the Kirchhoff theory has been formulated using the IFM (Patnaik *et al.* 1991) The element considers a transverse displacement and two rotations as degrees of freedom at each node. The performance of this element was compared with those obtained by force method (Przemieniecki 1968, Robinson 1973). Dhananjaya *et al.* (2009), proposed a new 8-node quadrilateral plate bending element for the analysis of thin and moderately thick plates using IFM and compared the results with those obtained from similar displacement based quadrilateral plate bending finite elements.

Research on thin (Kirchhoff theory) and moderately thick (Mindlin-Ressner theory) plates has attracted large community of research engineers and scientists for the past few decades. The Kirchhoff plate theory based plate bending elements consider C_1 continuity which rather difficult to adopt for higher order finite elements and neglect the effect of shear. However the Mindlin-Reissner theory based plate bending elements consider C_0 continuity, accounting effect of shear and avoid C_1 continuity. Quite a many quadrilateral plate bending elements are available in the literature. Few of them are reported by (Choi and Park 1999, Choi *et al.* 2002, Kim and Chang-Choi 2005, Kanber *et al.* 2006, Ozgan *et al.* 2007, Pian 1964, Tong 1970, Lee *et al.* 1982. Pian *et al.* 1982, Wanji *et al.* 1987, Dimitris *et al.* 1984, Darılmaz 2005 and Kutlu Darılmaz and Nahit Kumbasar 2006, Spilker 1982, Dhananjaya *et al.* 2009). Nine-node heterosis plate bending element is developed by (Huges and Martin 1978).

Almost void nine-node displacement-based finite element plate bending elements are available in the literature. Therefore it becomes necessary to develop force-based nine-node plate bending element for the analysis of thin and moderately thick plate bending problems. It also helps in

comparing the results of similar other plate bending elements available in the literature. Towards this goal, this paper proposes a new nine-node Lagrangian quadrilateral plate bending element (MQP9) to analyze the thin and moderately thick plate bending problems using IFM. The Mindlin-Reissner theory has been employed in the formulation which accounts for the shear deformation. This element considers three degrees of freedom namely a transverse displacement and two rotations at each node. Suitable displacement and stress-resultants fields are chosen over the element and element equilibrium and flexibility matrices are developed. The shear correction factor as suggested by Reissner (1945) has been considered in the formulation. Standard plate bending benchmark problems are analyzed using the proposed element MQP9 via Integrated Force Method. The results of this element are compared with those of similar displacement based quadrilateral elements. The results of proposed nine-node plate bending element (MQP9) are also compared with those of force-based eight-node plate bending element MQP8. The results of MQP9 are also compared with exact solutions. The proposed nine-node Lagrangian quadrilateral plate bending element has produced, in general, excellent results and can be successfully used to analyze the thin and moderately thick plate bending problems accounting shear deformation.

2. Formulation of element equilibrium and flexibility matrices

For the completeness, the basic theory of IFM is given in the appendix A.

In this section a brief formulation on the development of equilibrium and flexibility matrices of plate bending element using Integrated Force Method is described. The Mindlin – Reissner theory has been employed in the formulation. In the Mindlin – Reissner theory, a line that is straight and normal to mid-surface of the un-deformed plate remain straight but not necessarily normal to the mid-surface of the deformed plate. This leads to the following definition of the displacement components *u, v, w* in the *x, y, z* Cartesian coordinates system

$$u = -z\theta_x(x,y); \quad v = -z\theta_y(x,y); \quad w = w(x,y) \tag{1}$$

where

x, y are coordinates in the reference mid-surface

z is the coordinate through the thickness of the plate *t* with $-t/2 \leq z \leq t/2$

w is the transverse (lateral) displacement

θ_x, θ_y represent the rotations of the normal in **x-z** and **y-z** planes respectively

Engineering strains for the Mindlin-Reissner plate theory can be written as

$$\begin{Bmatrix} \varepsilon_x \\ \varepsilon_y \\ \gamma_{xy} \\ \gamma_{yz} \\ \gamma_{zx} \end{Bmatrix} = -\begin{Bmatrix} z\dfrac{\partial \theta_x}{\partial x} \\[2mm] z\dfrac{\partial \theta_y}{\partial y} \\[2mm] z\left(\dfrac{\partial \theta_x}{\partial y} + \dfrac{\partial \theta_y}{\partial x}\right) \\[2mm] \theta_y - \dfrac{\partial w}{\partial y} \\[2mm] \theta_x - \dfrac{\partial w}{\partial x} \end{Bmatrix} \tag{2}$$

H.R. Dhananjaya, P.C. Pandey, J. Nagabhushanam and Zainah Ibrahim

The stress - strain relations for an isotropic two-dimensional plate material is given by

$$\{\sigma\} = [C_{con}]\{\varepsilon\} \tag{3}$$

where $\{\sigma\} = [\sigma_s \quad \sigma_y \quad \tau_{xy} \quad \tau_{yz} \quad \tau_{xz}]^T$ = vector of stress components

$\{\varepsilon\} = [\varepsilon_x \quad \varepsilon_y \quad \gamma_{xy} \quad \gamma_{yz} \quad \gamma_{zx}]^T$ = vector of strain components

$$[C_{con}] = \text{constitutive matrix} = \frac{E}{(1-v^2)}\begin{bmatrix} 1 & v & 0 & 0 & 0 \\ v & 1 & 0 & 0 & 0 \\ 0 & 0 & \dfrac{(1-v)}{2} & 0 & 0 \\ 0 & 0 & 0 & \dfrac{(1-v)}{2} & 0 \\ 0 & 0 & 0 & 0 & \dfrac{(1-v)}{2} \end{bmatrix}$$

E = Young's modulus; v = Poisson's ratio

The stress-resultants for plates can be written as

$$M_x = \int_{-t/2}^{t/2} z\,\sigma_x dz$$

$$M_y = \int_{-t/2}^{t/2} z\,\sigma_y dz$$

$$M_{xy} = \int_{-t/2}^{t/2} z\,\tau_{xy} dz \tag{4}$$

$$Q_y = \int_{-t/2}^{t/2} \tau_{yz} dz$$

$$Q_x = \int_{-t/2}^{t/2} \tau_{xz} dz$$

Eqs. (2), (3) and (4) yield the moment-curvature relations as

$$\{M\} = [C_1]\{k\} \tag{5}$$

Where $\{M\}$ = vector of stress-resultants

$$= [M_x \quad M_y \quad M_{xy} \quad Q_y \quad Q_x]^T$$

$[C_1]$ = matrix relating stress-resultants to curvatures
$\{k\}$ = vector of curvatures

$$= \left[\frac{\partial\theta_x}{\partial x} \quad \frac{\partial\theta_y}{\partial y} \quad \frac{\partial\theta_x}{\partial y}+\frac{\partial\theta_y}{\partial x} \quad \theta_y-\frac{\partial w}{\partial y} \quad \theta_x-\frac{\partial w}{\partial x}\right]^T$$

From the Eq. (5), the curvature-moment relations can be written as

$$\{k\} = [C_1]^{-1}\{M\} = [H]\{M\} \tag{6}$$

where $[H] = [C_1]^{-1}$
        = matrix relating curvatures to stress-resultants

The matrix $[H]$ for the Mindlin - Reissner plate with Reissner's shear correction factor (Reissner 1945) of 5/6 can be written as

$$H = \frac{1}{D_1} \begin{bmatrix} 1 & -v & 0 & 0 & 0 \\ -v & 1 & 0 & 0 & 0 \\ 0 & 0 & 2(1+v) & 0 & 0 \\ 0 & 0 & 0 & \dfrac{t^2(1+v)}{5} & 0 \\ 0 & 0 & 0 & 0 & \dfrac{t^2(1+v)}{5} \end{bmatrix} \tag{7}$$

where $D_1 = Et^3/12$

The strain energy U_p of the elastic plate in bending and shear is written as

$$U_p = \iint 1/2 \left[M_x \frac{\partial \theta_x}{\partial x} + M_y \frac{\partial \theta_y}{\partial y} + M_{xy}\left(\frac{\partial \theta_x}{\partial y} + \frac{\partial \theta_y}{\partial x}\right) + Q_y\left(\theta_y - \frac{\partial w}{\partial y}\right) + Q_x\left(\theta_x - \frac{\partial w}{\partial x}\right) \right] dxdy \tag{8}$$

The vectors $\{M\}$ and $\{k\}$ for a discrete plate bending element can be expressed in matrix notations in terms of assumed stress-resultants and displacement fields respectively as

$$\{M\} = [\psi]\{F_e\} \tag{9}$$

$$\{k\} = [D_{op}][\phi_1]\{\alpha\} = [D_{op}][\phi]\{X_e\} \tag{10}$$

where

$[\psi]$ = matrix of polynomial terms for stress-resultant fields
$[F_e]$ = vector of force components of the discrete element
$[\phi_1]$ = matrix of polynomial terms for displacement fields
$[\phi]$ = $[\phi_1]\,[A]^{-1}$
$[A]$ = matrix formed by substituting the coordinates of the element nodes into the polynomial of displacement fields
$\{\alpha\}$ = coefficients of the displacement field polynomial
$\{X_e\}$ = vector of displacements of the discrete element

$$[D_{op}] = \text{differential operator matrix} = \begin{bmatrix} 0 & \dfrac{\partial}{\partial x} & 0 \\ 0 & 0 & \dfrac{\partial}{\partial y} \\ 0 & \dfrac{\partial}{\partial y} & \dfrac{\partial}{\partial x} \\ -\dfrac{\partial}{\partial y} & 0 & 1 \\ -\dfrac{\partial}{\partial x} & 1 & 0 \end{bmatrix}$$

Substituting Eqs. (9) and (10) into the Eq. (8), the strain energy for the discrete element can be

expressed as

$$U_p = 1/2\{X_e\}^T[B_e]\{F_e\} \tag{11}$$

where $[B_e]$ represents the element equilibrium matrix and is given by

$$[B_e] = \iint[\phi]^T[D_{op}]^T[\psi]dxdy \tag{12}$$

The complementary strain energy for the elastic plate in bending and shear is expressed as

$$U_c = \iint 1/2 \frac{1}{D_1}\left[M_x^2 + M_y^2 - 2\nu M_x M_y + 2(1+\nu)M_{xy}^2 + Q_y^2\frac{t^2(1+\nu)}{5} + Q_x^2\frac{t^2(1+\nu)}{5}\right]dxdy$$

Using the Eq. (7), the complementary strain energy for the discrete element is written as

$$U_c = 1/2\{F_e\}^T[G_e]\{F_e\} \tag{13}$$

where $[G_e]$ represents the element flexibility matrix and is given by

$$[G_e] = \iint[\psi]^T[H]\{\psi\}dxdy \tag{14}$$

The Eqs. (12) and (14) are used to obtain element equilibrium matrix $[B_e]$ and element flexibility matrix $[G_e]$ respectively. These element matrices $[B_e]$ and $[G_e]$ of all elements are assembled to obtain the global equilibrium matrix $[B]$ and global flexibility matrix $[G]$ of the structure and they are used to setup the IFM governing equation to analyze the plate problems by IFM.

2.1 Displacement and stress-resultant fields

The assumed polynomials for displacement fields should satisfy the convergence requirements. Displacement fields for Kirchhoff theory based plate bending elements should satisfy the C_1 continuity while that for the Mindlin-Reissner theory based plate bending elements should satisfy the C_0 continuity. The single displacement field w representing transverse displacement is enough in the Kirchhoff theory based plate bending elements as other two rotations θ_x and θ_y are expressed in terms of the transverse displacement w itself. However independent displacement fields are required to be assumed for transverse displacement w and rotations for θ_x and θ_y to satisfy the C_0 continuity, in the Mindlin-Reissner plate theory.

The IFM allows describing polynomials for stress-resultant fields. The stress-resultant fields should be expressed in polynomial terms along with generalized force parameters/components. The
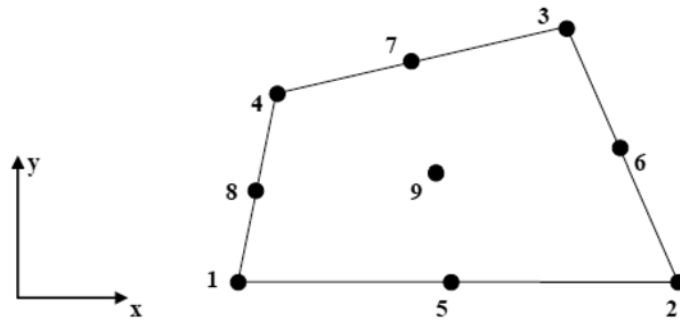

Fig. 1 A typical nine-node Lagrangian quadrilateral plate bending element

assumed stress-resultant fields should satisfy the plate equilibrium equations. Further the generalized force parameters/components in stress-resultant fields should be independent of each other which ensure the kinematic stability of the element model in IFM.

A typical nine-node Lagrangian quadrilateral plate bending element is shown in the Fig. 1. Three degrees of freedom namely, the transverse displacement (w) and two rotations (θ_x and θ_y) are considered at each node of this element. The Eq. (15) show the assumed independent displacement fields for the transverse displacement (w) and two rotations (θ_x and θ_y).

$$w = \alpha_1 + \alpha_2 x + \alpha_3 y + \alpha_4 x^2 + \alpha_5 xy + \alpha_6 y^2 + \alpha_7 x^2 y + \alpha_8 xy^2 + \alpha_9 x^2 y^2$$

$$\theta_x = \alpha_{10} + \alpha_{11} x + \alpha_{12} y + \alpha_{13} x^2 + \alpha_{14} xy + \alpha_{15} y^2 + \alpha_{16} x^2 y + \alpha_{17} xy^2 + \alpha_{18} x^2 y^2$$

$$\theta_y = \alpha_{19} + \alpha_{20} x + \alpha_{21} y + \alpha_{22} x^2 + \alpha_{23} xy + \alpha_{24} y^2 + \alpha_{25} x^2 y + \alpha_{26} xy^2 + \alpha_{27} x^2 y^2 \tag{15}$$

Eq. (16) shows the assumed stress-resultant fields in terms of generalized independent forces $F_1, F_2 \dots F_{24}$ for this 9-node Lagrangian quadrilateral plate bending element.

$$M_x = F_1 + F_2 x + F_3 y + F_4 x^2 + F_5 xy + F_6 y^2 + F_7 x^2 y + F_8 xy^2$$

$$M_y = F_9 + F_{10} x + F_{11} y + F_{12} x^2 + F_{13} xy + F_{14} y^2 + F_{15} x^2 y + F_{16} xy^2$$

$$M_{xy} = F_{17} + F_{18} x + F_{19} y + F_{20} x^2 + F_{21} xy + F_{22} y^2 + F_{23} x^2 y + F_{24} xy^2$$

$$Q_y = (F_{11} + F_{18}) + (F_{13} + 2F_{20})x + (2F_{14} + F_{21})y + F_{15} x^2 + 2(F_{16} + F_{23})xy + F_{24} y^2$$

$$Q_x = (F_2 + F_{19}) + (2F_4 + F_{21})x + (F_5 + 2F_{22})y + F_{23} x^2 + 2(F_7 + F_{24})xy + F_8 y^2 \tag{16}$$

Substituting displacement and stress-resultant fields given by Eqs. (15) and (16) along with the Eq. (7) into Eqs. (12) and (14), element equilibrium and flexibility matrices for this nine-node Lagrangian element are obtained

3. Numerical tests and discussions

The performance of the proposed element MQP9 is illustrated by analyzing the following standard benchmark plate bending example problems available in the literature.

1. A square thin plate ($t/L = 0.01$) with simply supported/clamped boundary conditions subjected to uniform load/central point load. The parameters of the problem are: size of the plate = 100 × 100, $t = 1$, $E = 1 \times 10^7$, $v = 0.3$, $q = 10$, $P = 400$ (Spilker 1982).

2. A rectangular thin plate (aspect ratio = 2 or 3) with simply supported/clamped boundary conditions subjected to uniform load. The parameters of the problem are: size of the plate = 200 × 100 or 300 × 100, $t = 1$, $E = 1 \times 10^7$, $v = 0.3$, $q = 10$. (Spilker 1982).

3. A square moderately thick plate ($t/L = 0.1$) with simply supported/clamped boundary conditions subjected to uniform load/central point load. The parameters of the problem are: size of the plate = 100 × 100, $t = 10$, $E = 2 \times 10^5$, $v = 0.3$, $q = 10$, $P = 400$.

4. The Morley's plate problem (Fig. 2) - the parameters of the problems are: $L = 100$, $B = 100$, $t = 1$, $E = 1.092 \times 10^6$, $v = 0.3$ and $q = 1$, inclination of the plate $\theta = 30^0$, $w = 0$ on all boundaries (Morley 1963).

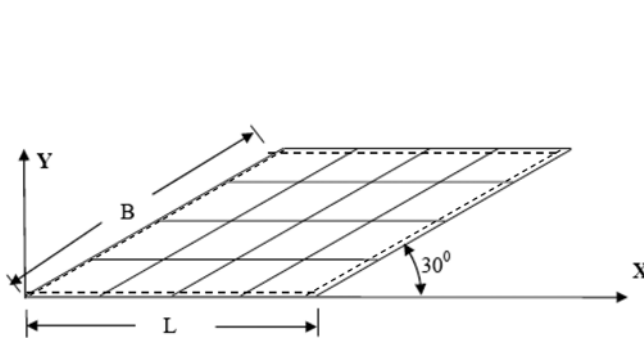5. The Razzaque's plate problem (Fig. 3). The parameters of the problems are: $L = 100$, $B = 100$, t

Fig. 2 Morley's plate: $L = 100$, $B = 100$, $t = 1$, $E = 1.092 \times 10^6$, $v = 0.3$ and $q = 1$, inclination of the plate $\theta = 30^0$, $w = 0$ on all sides of the plate
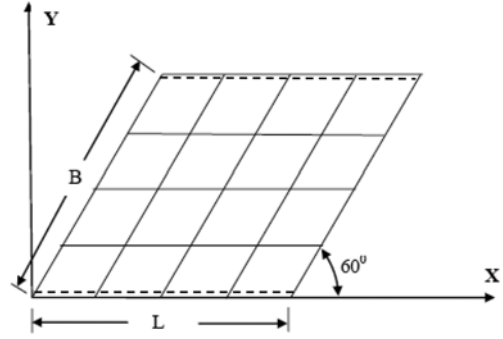
Fig. 3 Razzaque's plate: $L = 100$, $B = 100$, $t = 1$, $E = 1.092 \times 10^6$, $v = 0.3$ and $q = 1$, inclination of the plate $\theta = 60^0$ (Two opposite edges simply supported while other two free)

= 1, $E = 1.092 \times 10^6$, $v = 0.3$ and $q = 1$, inclination of the plate $\theta = 60^0$ (Razzaque 1973).

These example problems are analyzed for different grid sizes using the proposed element MQP9 to estimate central deflections and bending moments. The results of the proposed element MQP9 are compared with those of displacement-based similar quadrilateral plate bending elements QH1, QH2, QH3 and QH4 available in literature (Spilker 1982), and those computed using similar elements in commercial software packages NISA (NISA version 9.3). The results are also compared with those from force-based 8-node quadrilateral plate bending element MQP8 (Dhananjaya *et al.* 2009). The results are also compared with the exact solutions given in the references (Timoshenko 1957, Jane and Tessler 2000) for thin plates and moderately thick plates respectively. The exact solutions for central deflection and bending moment of square plates are given in the Table B1 (Appendix B, (Jane and Tessler 2000)). The results of the proposed element MQP9 for skew plates with various boundary conditions are compared with the exact solutions given in references (Morley 1963, Razzaque 1973).

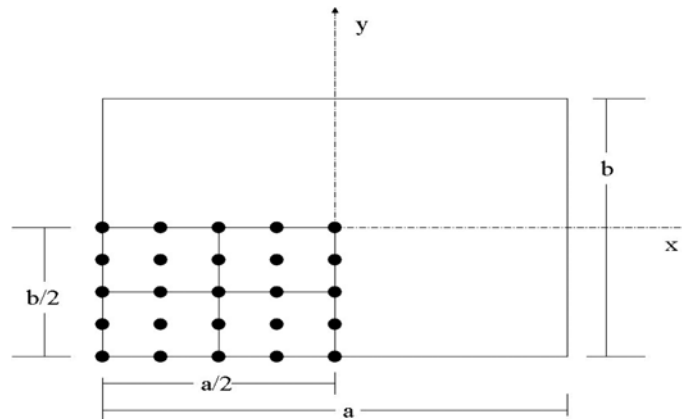Due to symmetry of the plate, loading and boundary conditions, the square or rectangular thin/

Fig. 4 A typical mesh (2 × 2) in one quadrant of the rectangular plate

thick plate example problems 1-3 are analyzed considering one quadrant of the plate. A typical mesh (2×2) in one quadrant of the plate for the element MQP9 is shown in the Fig. 4.

3.1 Square thin plate problems (Example Problem 1)

Normalized central deflections and moments for a simply supported square thin ($t/L = 0.01$) plate subjected to uniform load (example problem 1) are summarized in the Tables 1 and 2 respectively. The corresponding converging trends are shown in Figs. 5 and 6 respectively.

Tables 3 and 4 respectively show normalized central deflections and moments for a clamped square thin ($t/L = 0.01$) plate subjected to uniform load (example problem 1). The corresponding

Table 1 Normalized central deflection for simply supported thin square plate with uniform load (Example Problem 1) ($t/L = 0.01$)

Elements	QH1	QH2	QH3	QH4	MQP8	MQP9
1×1	0.955	0.890	0.900	0.835	0.954	0.981
2×2	1.000	0.985	0.990	0.980	1.000	1.000
3×3	1.000	0.990	0.990	0.990	1.000	1.000
4×4	1.000	0.990	0.990	0.990	1.000	1.000

Table 2 Normalized central moment for simply supported thin square plate with uniform load (Example Problem 1) ($t/L = 0.01$)

Elements	QH1	QH2	QH3	QH4	MQP8	MQP9
1×1	0.580	0.560	0.640	0.700	0.475	0.871
2×2	0.980	1.015	0.965	1.010	1.010	1.022
3×3	0.990	1.030	0.985	1.006	1.006	0.997
4×4	0.990	1.020	0.990	1.006	1.006	1.001

Table 3 Normalized central deflection for clamped thin square plate with uniform load (Example Problem 1) ($t/L = 0.01$)

Elements	QH1	QH2	QH3	QH4	MQP8	MQP9
1×1	1.170	0.900	0.990	0.440	1.153	1.099
2×2	0.990	0.955	0.940	0.830	0.994	1.010
3×3	1.000	0.980	0.985	0.935	1.003	1.005
4×4	1.000	0.990	0.990	0.970	1.003	1.003

Table 4 Normalized central moment for clamped thin square plate with uniform load (Example Problem 1) ($t/L = 0.01$)

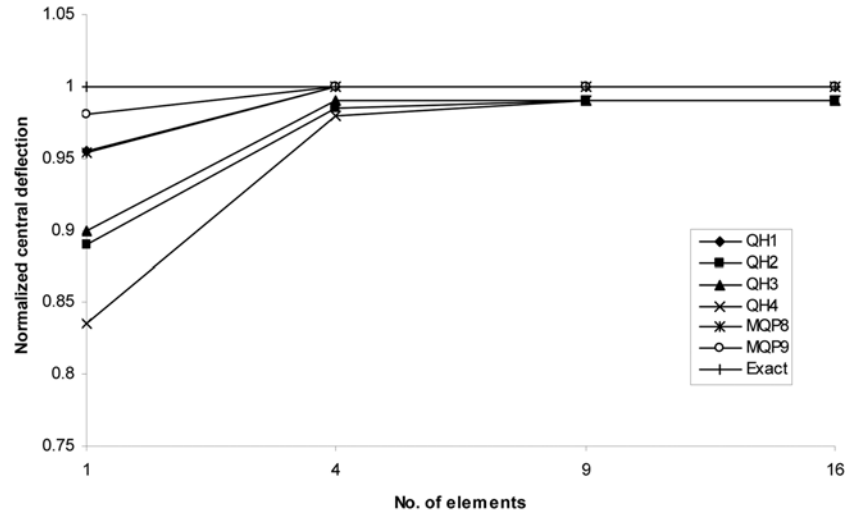| Elements	QH1	QH2	QH3	QH4	MQP8	MQP9
1×1	0.950	0.570	0.790	0.940	0.836	0.707
2×2	0.820	0.780	0.730	0.870	0.790	1.033
3×3	0.990	0.990	0.980	0.990	0.970	0.992
4×4	0.990	1.010	0.980	0.990	0.980	0.996

Fig. 5 Normalized central deflection for simply supported thin square plate with uniform load ($t/L = 0.01$, Example Problem 1)
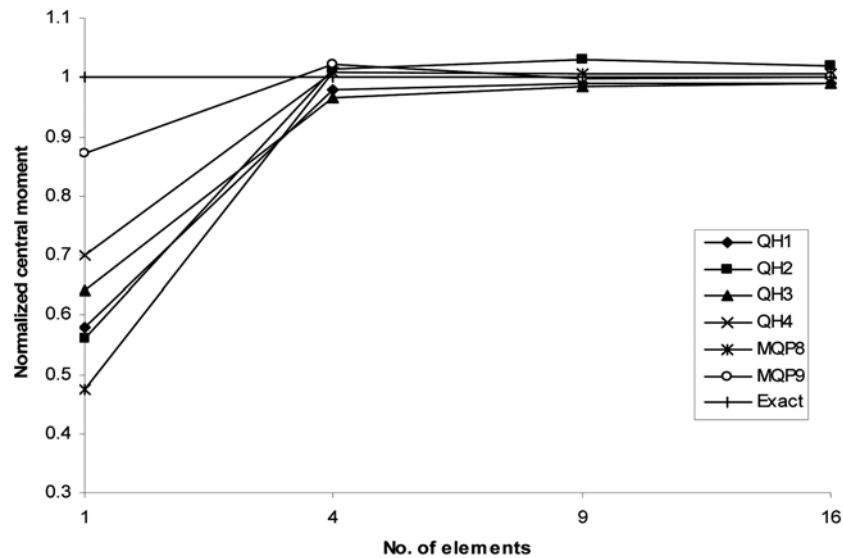

Fig. 6 Normalized central moment for simply supported thin square plate with uniform load ($t/L = 0.01$, Example Problem 1)

converging trends are shown in Fig. 7 and 8 respectively.

Normalized central deflections for simply supported thin square ($t/L = 0.01$) plate and clamped thin square ($t/L = 0.01$) plate with central point load (example problem 1) are summarized in Tables 5 and 6. The corresponding converging trends are shown in Figs. 9 and 10.

The results of the proposed element MQP9 in Tables 1-6 are better, in general, compared to all other elements QH1, QH2, QH3, QH4 and MQP8. Figs. 5-10 indicate that results of MQP9 are fast converging to the exact solutions.
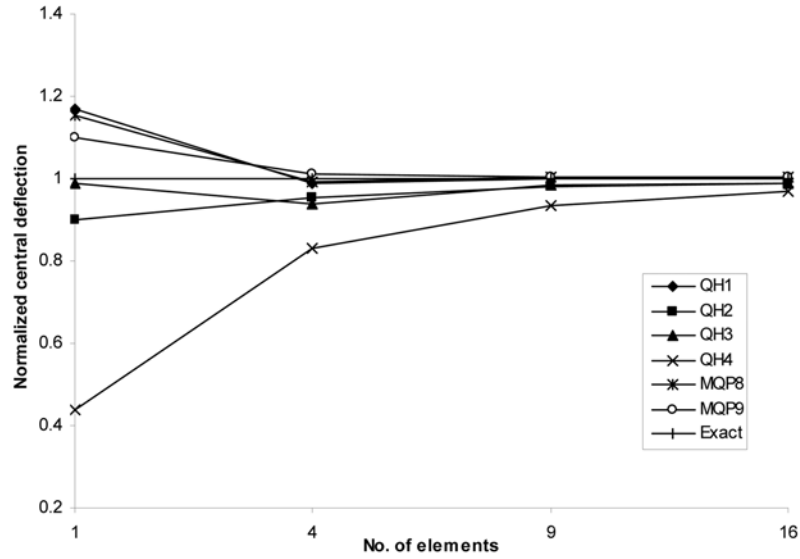
Fig. 7 Normalized central deflection for clamped thin square plate with uniform load ($t/L = 0.01$, Example Problem 1)
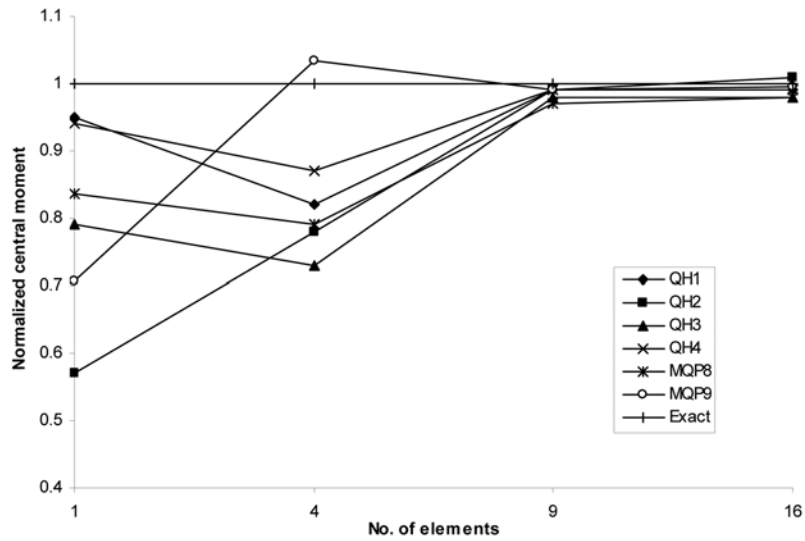

Fig. 8 Normalized central moment for clamped thin square plate with uniform load ($t/L = 0.01$, Example Problem 1)

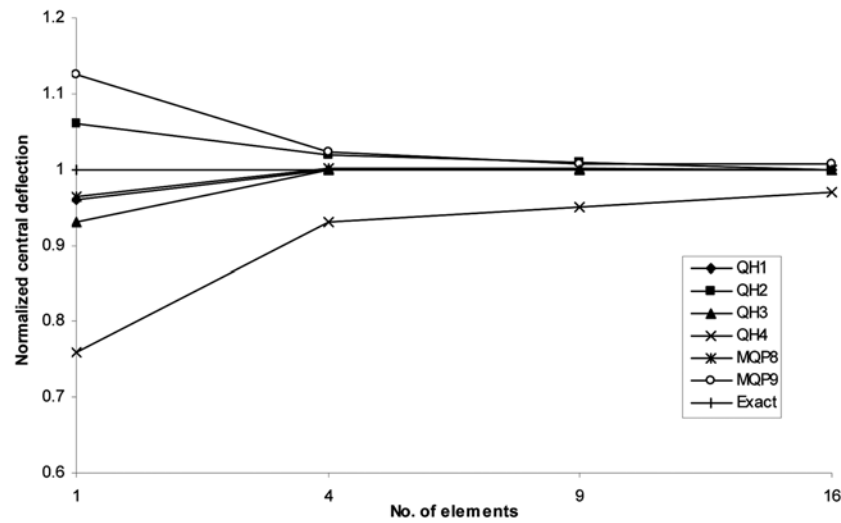Table 5 Normalized central deflection for simply supported thin square plate with central point load (Example Problem 1) ($t/L = 0.01$)

Elements	QH1	QH2	QH3	QH4	MQP8	MQP9
1 × 1	0.96	1.06	0.93	0.76	0.963	1.125
2 × 2	1.00	1.02	1.00	0.93	1.001	1.023
3 × 3	1.00	1.01	1.00	0.95	1.001	1.008
4 × 4	1.00	1.00	1.00	0.97	1.000	1.007

Table 6 Normalized central deflection for clamped thin square plate with central point load (Example Problem 1) (*t*/*L* = 0.01)

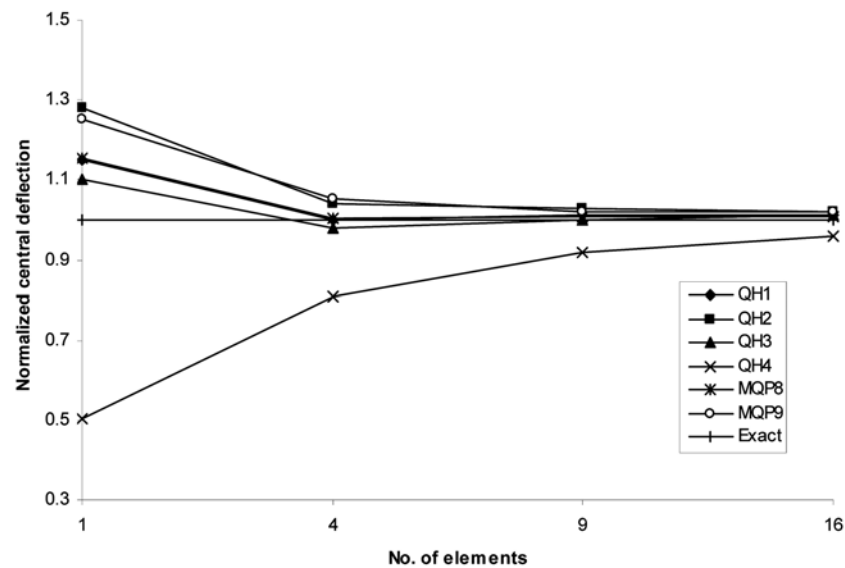| Elements	QH1	QH2	QH3	QH4	MQP8	MQP9
1 × 1	1.15	1.28	1.10	0.505	1.154	1.251
2 × 2	1.00	1.04	0.98	0.81	1.002	1.051
3 × 3	1.01	1.03	1.00	0.92	1.009	1.021
4 × 4	1.01	1.02	1.01	0.96	1.009	1.018

Fig. 9 Normalized central deflection for simply supported thin square plate with central point load (*t*/*L* = 0.01, Example Problem 1)

Fig. 10 Normalized central deflection for clamped thin square plate with central point load (*t*/*L* = 0.01, Example Problem 1)

Table 7 Normalized central deflection for a simply supported thin rectangular plate (aspect ratio = 2) with uniform load (Example Problem 2)

Elements	QH1	QH2	QH3	QH4	MQP8	MQP9
1 × 1	0.975	0.870	0.910	0.855	0.960	0.975
2 × 2	1.000	0.990	1.010	0.980	1.000	0.999
3 × 3	1.000	1.000	1.000	0.990	1.000	1.002
4 × 4	1.000	1.000	1.000	0.995	1.000	1.000

Table 8 Normalized central moment M_x for a simply supported thin rectangular plate (aspect ratio = 2) with uniform load (Example Problem 2)

Elements	QH1	QH2	QH3	QH4	MQP8	MQP9
1 × 1	0.720	1.800	1.020	1.090	0.410	1.079
2 × 2	1.040	1.550	0.970	0.980	0.940	0.922
3 × 3	1.020	1.140	0.980	0.985	0.970	0.983
4 × 4	1.010	1.090	0.990	0.990	0.980	1.002

Table 9 Normalized central moment M_y for a simply supported thin rectangular plate (aspect ratio = 2) with uniform load (Example Problem 2)

Elements	QH1	QH2	QH3	QH4	MQP8	MQP9
1 × 1	0.640	0.860	0.890	0.690	0.520	0.852
2 × 2	1.080	1.060	1.070	1.100	1.010	1.028
3 × 3	1.020	1.025	1.025	1.030	1.000	1.001
4 × 4	1.010	1.015	1.015	1.020	1.000	1.000

3.2 Rectangular thin plate problems with aspect ratio 2 and 3 (Example Problem 2)

Normalized central deflections and moments for a simply supported rectangular thin plate with the aspect ratio 2, subjected to uniform load (example problem 2) are summarized in the Tables 7-9. The corresponding converging trends are shown in Figs. 11-13.

Tables 10 and 11 respectively show normalized central deflections for a simply supported and clamped thin rectangular plate with the aspect ratios 3 subjected to uniform load (example problem 2). The corresponding converging trends are depicted in Figs. 14 and 15 respectively. Here also Tables 7-11 and corresponding Figs. 11-15 indicate that the proposed element MQP9 performs better, in general, compared to other elements considered.

3.3 Square thick plate problem (Example Problem 3)

Central deflections and moments for a simply supported square thick ($t/L = 0.1$) plate subjected to uniform load (example problem 3) are given in the Tables 12 and 13 respectively. The corresponding converging trends are shown in Figs. 16 and 17 respectively.

Tables 14 and 15 respectively show central deflections and moments for a clamped square thick ($t/L = 0.1$) plate subjected to uniform load (example problem 3). The corresponding converging trends
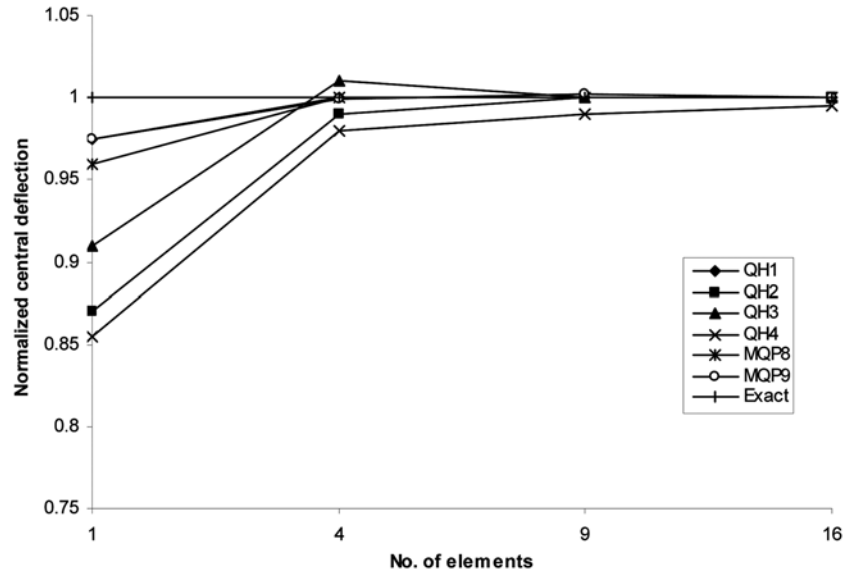
Fig. 11 Normalized central deflection for a simply supported thin rectangular plate (aspect ratio = 2) with uniform load (t/L = 0.01, Example Problem 2)
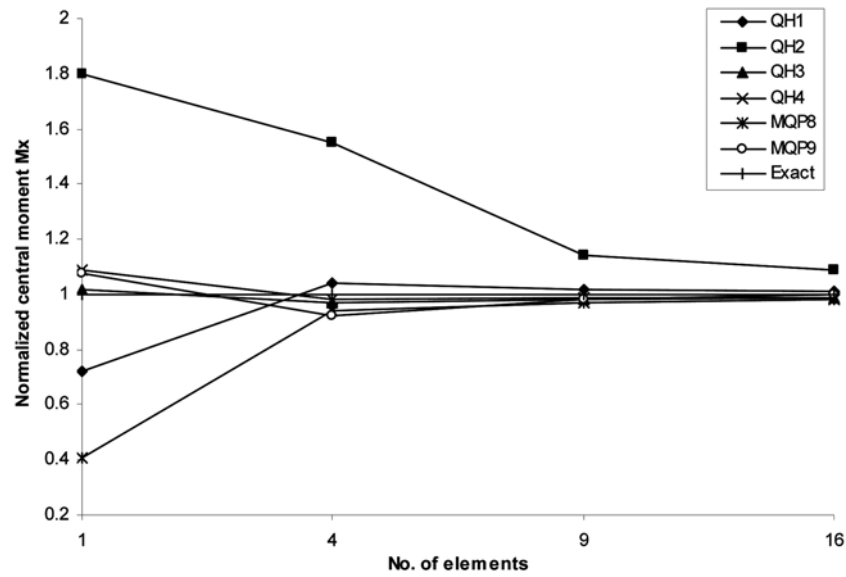

Fig. 12 Normalized central moment M_x for a simply supported thin rectangular plate (aspect ratio = 2) with uniform load (t/L = 0.01, Example Problem 2)

are shown in Figs. 18 and 19 respectively.

In both the above cases, the proposed element MQP9 has performed better, in general, compare to other elements considered.
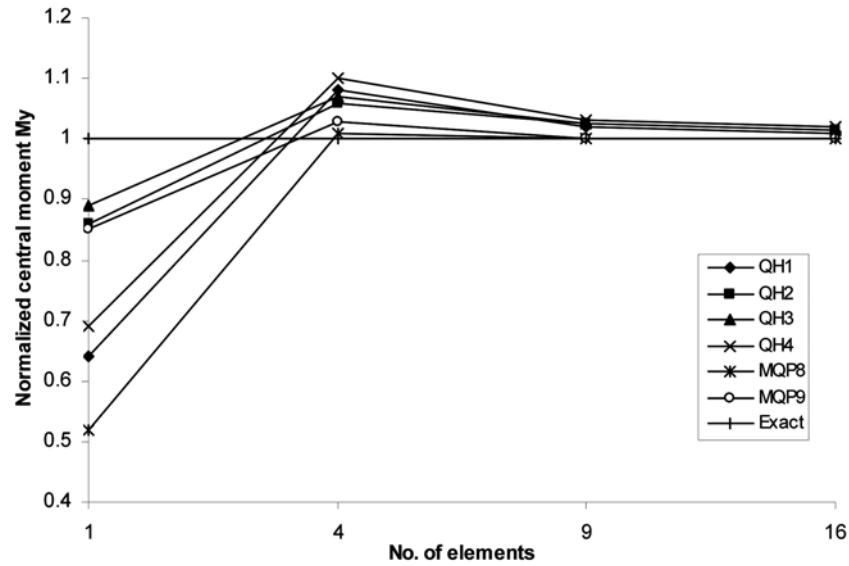
Fig. 13 Normalized central moment M_y for a simply supported thin rectangular plate (aspect ratio = 2) with uniform load (t/L = 0.01, Example Problem 2)

Table 10 Normalized central deflection for a simply supported thin rectangular plate (aspect ratio = 3) with uniform load (Example Problem 2)

Elements	QH1	QH2	QH3	QH4	MQP8	MQP9
1 × 1	1.020	0.865	0.920	0.890	0.990	1.016
2 × 2	1.006	1.075	1.028	0.980	1.000	0.998
3 × 3	1.000	1.006	1.008	0.985	1.000	1.001
4 × 4	1.000	1.000	1.000	0.990	1.000	1.000

Table 11 Normalized central deflection for a clamped thin rectangular plate (aspect ratio=3) with uniform load (Example Problem 2)

Elements	QH1	QH2	QH3	QH4	MQP8	MQP9
1 × 1	1.19	1.10	1.08	0.82	0.90	1.044
2 × 2	1.09	1.05	0.97	0.81	0.90	1.008
3 × 3	1.05	1.00	0.94	0.85	1.01	1.009
4 × 4	1.02	0.99	0.97	0.89	1.01	1.007

3.4 Morley's plate problem (Example Problem 4)

The central deflections of the Morley's plate (skew plate, $\theta = 30^0$, example problem 4) for various grid sizes, subjected to uniform load are plotted and converging trends are shown in Fig. 20. The proposed element MQP9 is found to be converging continuously faster towards the exact solution.
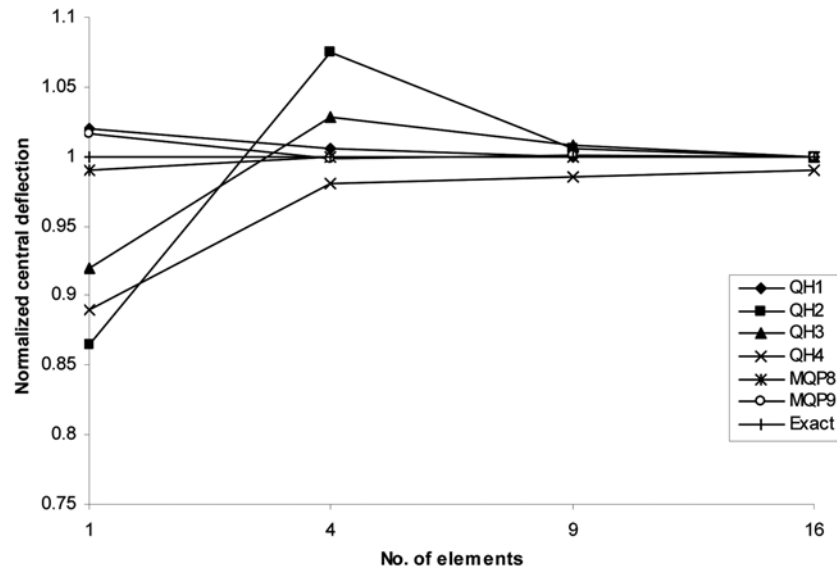
Fig. 14 Normalized central deflection for a simply supported thin rectangular plate (aspect ratio = 3) with uniform load (*t/L* = 0.01, Example Problem 2)

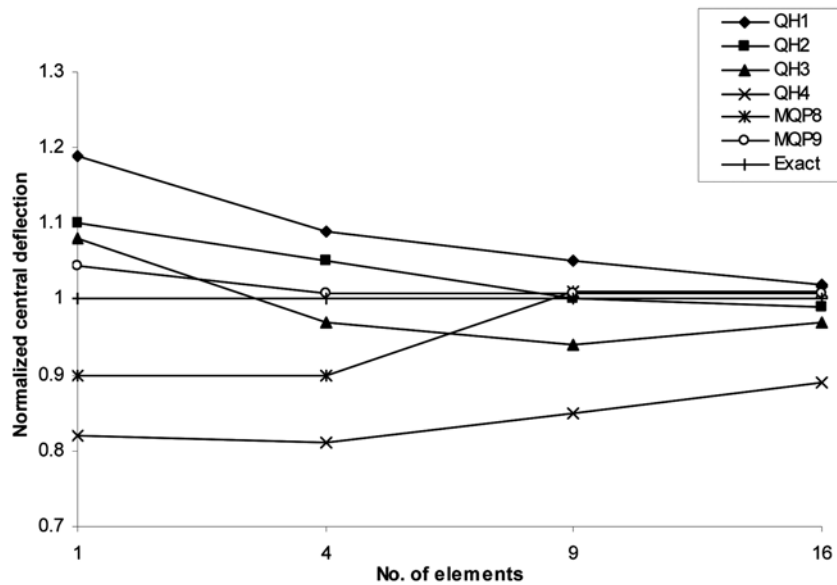
Fig. 15 Normalized central deflection for a clamped thin rectangular plate (aspect ratio = 3) with uniform load (*t/L* = 0.01, Example Problem 2)

3.5 Razzaque's plate problem (Example Problem 5)

Central deflections for various grid sizes of the Razzaque's plate (skew plate, $\theta = 60^0$, example problem 5) subjected to uniform load are plotted and converging trends are shown in Fig. 21. The Fig. 21 indicates that the proposed element MQP9 is converging faster towards the exact solution.
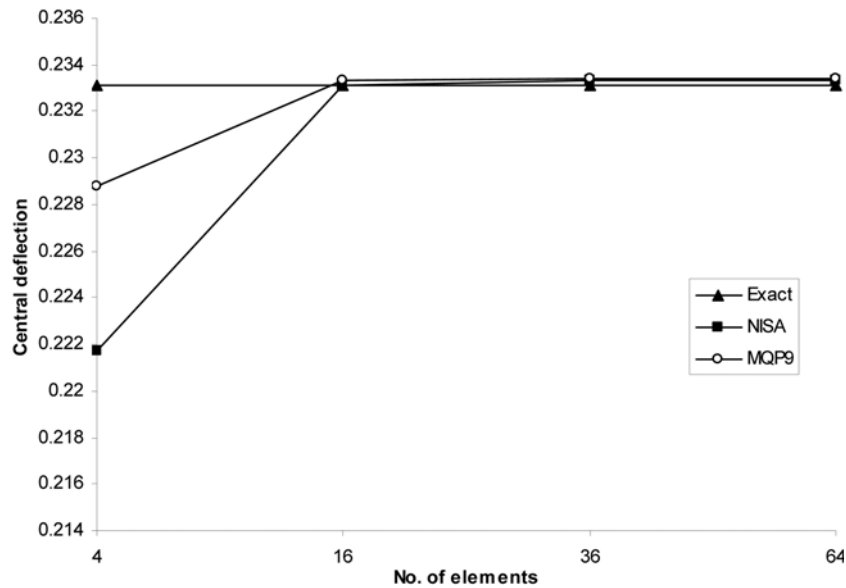
Table 12 Central deflection for simply supported thick square plate with uniform load (Example Problem 3)

Elements	MQP9	NISA
2 × 2	0.2288	0.2217
4 × 4	0.2333	0.2331
6 × 6	0.2334	0.2333
8 × 8	0.2334	0.2333
Exact	0.2331	

Table 13 Central moment for simply supported thick square plate with uniform load (Example Problem 3)

Elements	MQP9	NISA
2 × 2	4123.60	6703.07
4 × 4	4883.05	5162.60
6 × 6	4824.50	4946.61
8 × 8	4794.32	4875.57
Exact	4790.00	

Fig. 16 Central deflection for simply supported thick square plate with uniform load ($t/L = 0.1$, Example Problem 3)

3.6 Shear locking test

To study the shear locking behavior of the proposed element MQP9, the square plate of various thickness-span ratios ($t/L = 0.00001$, 0.0001, 0.001, 0.01 and 0.1) with simply supported and clamped boundary conditions subjected to uniform load is considered. The parameters of the problem
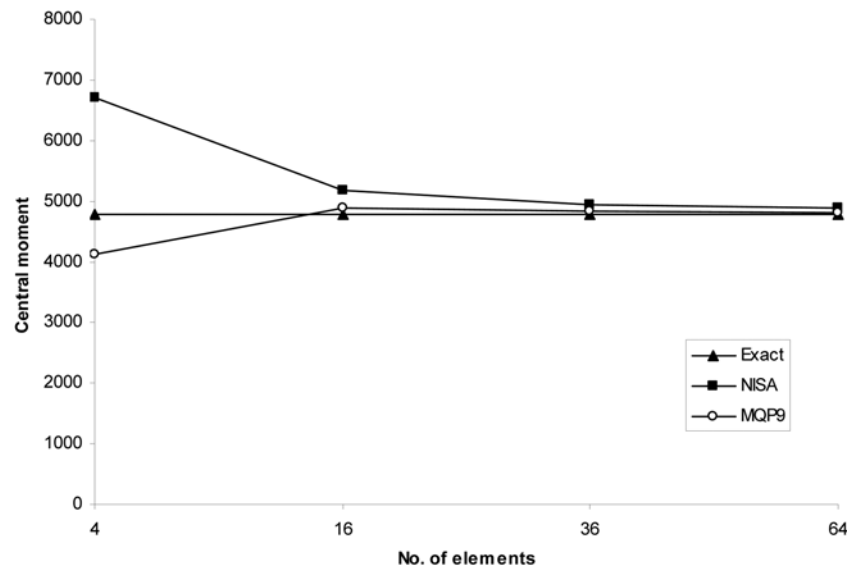
Fig. 17 Central moment for simply supported thick square plate with uniform load ($t/L = 0.1$, Example Problem 3)

Table 14 Central deflection for clamped thick square plate with uniform load (Example Problem 3)

Elements	MQP9	NISA
2×2	0.0866	0.0956
4×4	0.0824	0.0820
6×6	0.0823	0.0822
8×8	0.0822	0.0822
Exact	0.0819	

Table 15 Central moment for clamped thick square plate with uniform load (Example Problem 3)

Elements	MQP9	NISA
2×2	1690.80	4875.00
4×4	2400.75	2735.18
6×6	2347.12	2484.82
8×8	2328.2	2408.99
Exact	2310.0	

considered are: $L = 50$, $B = 50$, $t = 5$, 0.5, 0.005, 0.005, 0.0005, $E = 2 \times 10^5$, $v = 0.3$, $q = 1$ and $P = 10$. One quadrant of this plate problem is analyzed using proposed element MQP9 for the mesh size (4×4) to estimate the central deflections and moments. The exact central deflections and moments are calculated from the Kirchhoff theory (Timoshenko and Krieger 1959) and Mindlin theory (Jane and Tessler 2000, Table B1) solutions for thin and moderately thick plate bending
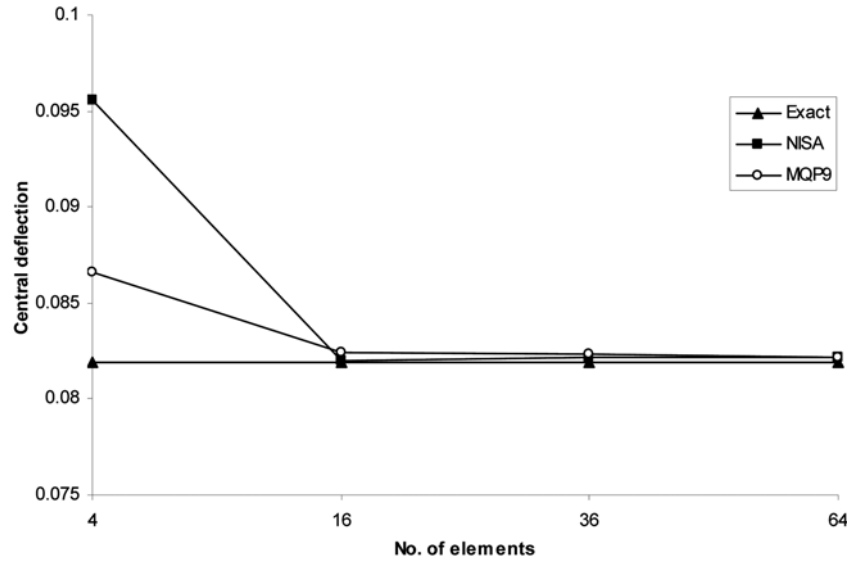
Fig. 18 Central deflection for clamped thick square plate with uniform load ($t/L = 0.1$, Example Problem 3)

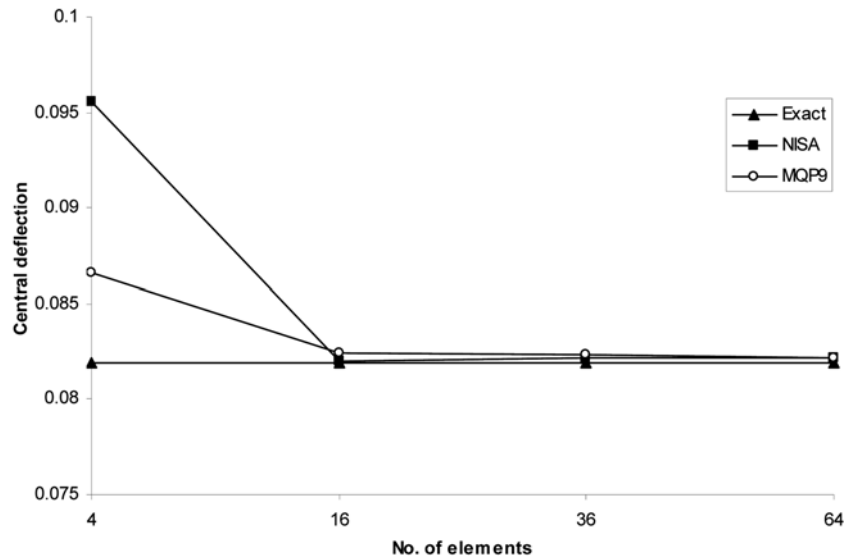
Fig. 19 Central moment for clamped thick square plate with uniform load ($t/L = 0.1$, Example Problem 3)

problems respectively. The central deflections and moments of simply supported plate with uniform for various thickness-span ratios by the proposed element are plotted in the Figs. 22 and 23 respectively. Figs. 24 and 25 respectively show central deflections and moments for the clamped plate subjected to uniform load. The results indicate that the proposed element MQP9 is free from the shear locking and performs excellent in both thin and moderately thick plate bending situations.

In all the example problems 1-5, Tables 1-15 and Figs. 5-25 indicate that the proposed nine-node Lagrangian quadrilateral plate bending element (MQP9) has yielded, in general, excellent results. These results of MQP9 are compared with those of similar displacement-based quadrilateral plate
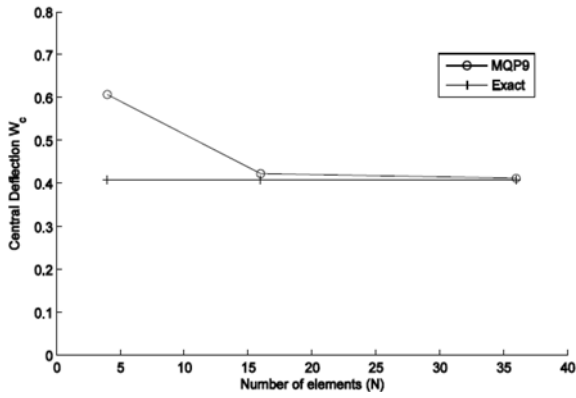
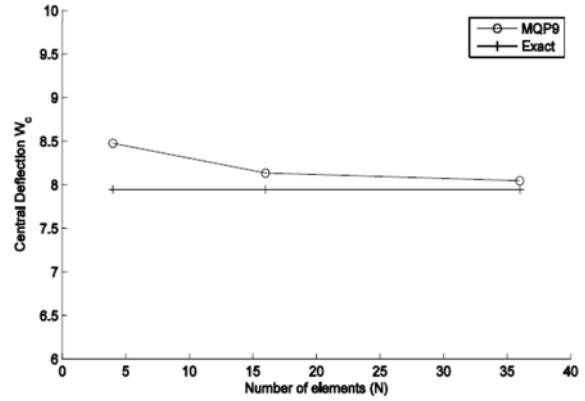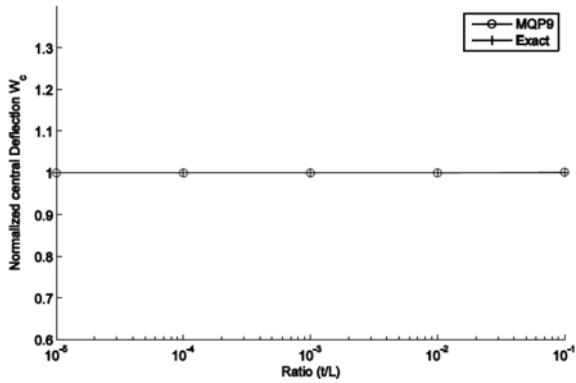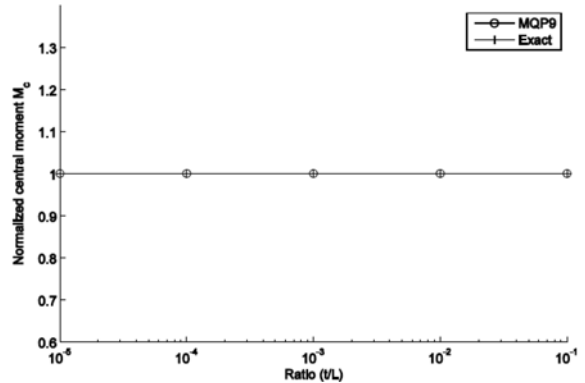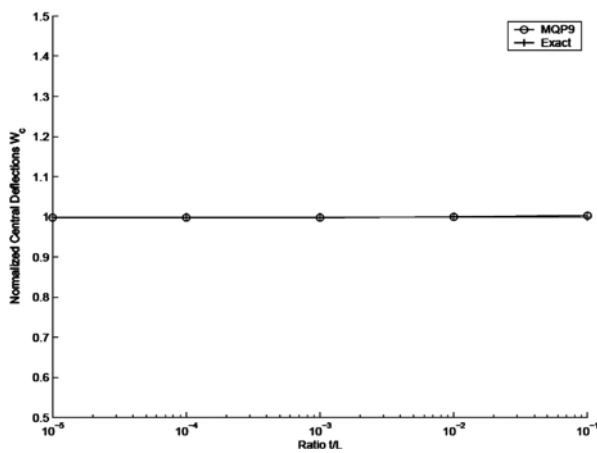Fig. 20 Central deflection for Morley's plate (Example Problem 4)

Fig. 21 Central deflection for Razzaque's plate (Example Problem 5)

Fig. 22 Normalized central deflections of simply supported plate with uniform load for various thickness-span ratios (t/L = 0.00001, 0.0001, 0.001, 0.01 and 0.1)

Fig. 23 Normalized central moments of simply supported plate with uniform load for various thickness-span ratios (t/L = 0.00001, 0.0001, 0.001, 0.01 and 0.1)

Fig. 24 Normalized central deflections of simply supported plate with uniform load for various thickness-span ratios (t/L = 0.00001, 0.0001, 0.001, 0.01 and 0.1)

Fig. 25 Normalized central moments of clamped plate with uniform load for various thickness-span ratios (t/L = 0.00001, 0.0001, 0.001, 0.01 and 0.1)

bending elements QH1, QH2, QH3, QH4 and NISA8 (from NISA commercial software version 9.3) considered from literature. The results of MQP9 are also compared with those of 8-node force-based quadrilateral plate bending element MQP8. These results are better, in general, compare to 8-node force-based quadrilateral plate bending element MQP8 and other displacement-based quadrilateral plate bending elements considered. The results of proposed nine-node Lagrangian quadrilateral plate bending element (MQP9) are also compared with exact solutions. These results of proposed element MQP9 are fast converging to the exact solutions.

4. Conclusions

Based on the Mindlin-Reissner theory, a new nine-node Lagrangian quadrilateral plate bending element (MQP9) has been proposed using Integrated Force Method to analyze the thin and moderately thick plate bending problems. The proposed element MQP9 considers three degrees of freedom namely a transverse displacement w and two rotations (θ_x and θ_y) at each node.

Various standard plate bending benchmark problems have been analyzed using this new proposed element (MQP9) via Integrated Force Method. The proposed element (MQP9) has yielded, in general, the excellent results in all the example problems considered and in comparison these results are better than the displacement-based similar quadrilateral plate bending elements considered from literature, Results of the proposed element (MQP9) are also better, in general, than force-based eight node quadrilateral plate bending element (MQP8).

Further the proposed element MQP9 is free from spurious energy modes and it does not lock under thin plate bending situations. Hence the same element can be used to analyze both thin and moderately thick plate bending problems. This proposed new nine-node Lagrangian quadrilateral plate bending element (MQP9) becomes an alternative higher order force-based plate bending element to analyze thin and moderately thick plate bending problems and to compare results of displacement-based similar elements available in the literature.

References

Choi, C.K. and Park, Y.M. (1999), "Quadratic NMS Mindlin-plate-bending element", *Int. J. Numer. Meth. Eng.*, **46**(8), 1273-1289.

Choi, C.K., Lee, T.Y. and Chung, K.Y. (2002), "Direct modification for nonconforming elements with drilling DOF", *Int. J. Numer. Meth. Eng.,* **55**(12), 1463-1476.

Chen, W.J. and Cheung, Y.K. (1987), "A new approach for the hybrid element method", *Int. J. Numer. Meth. Eng.*, **24**, 1697-1709.

Darýlmaz, K. (2005), "An assumed-stress finite element for static and free vibration analysis of Reissner-Mindlin plates", *Struct. Eng. Mech.,* **19**(2), 199-215.

Darýlmaz, K. and Kumbasar, N. (2006), "An 8-node assumed stress hybrid element for analysis of shells", *Comput. Struct.*, **84**, 1990-2000.

Dhananjaya, H.R., Pandey, P.C. and Nagabhushanam, J. (2009), "New eight node serendipity quadrilateral plate bending element for thin and moderately thick plates using Integrated Force Method"*, Struct. Eng. Mech.* **33**(4), 485-502.

Dimitris, K, Hung, L.T., and Atluri, S.N. (1984), "Mixed finite element models for plate bending analysis, A new element and its applications", *Comput. Struct.*, **19**(4), 565-581.

Hughes, T.J.R. and Cohen, M. (1978), "The 'heterosis' finite element for plate bending", *Comput. Struct.,* **9**(5),

445-450.

Kaljevic, I., Patnaik, S.N. and Hopkins, D.A. (1996), "Development of finite elements for two- dimensional structural analysis using Integrated Force Method", *Comput. Struct.,* **59**(4), 691-706.

Kaljevic, I., Patnaik, S.N. and Hopkins, D.A. (1996), "Three dimensional structural analysis by Integrated Force Method", *Comput. Struct.*, **58**(5), 869-886.

Kanber, B. and Bozkurt. Y. (2006), "Finite element analysis of elasto-plastic plate bending problems using transition rectangular plate elements", *Acta Mechanica Sinica*, **22**, 355-365.

Kaneko, L., Lawo, H. and Thierauf G. (1983), "On computational procedures for the force method", *Int. J. Numer. Meth. Eng.*, **18**, 1469-1495.

Krishnam Raju, N.R.B. and Nagabhushanam, J. (2000), "Non-linear structural analysis using integrated force method", *Sadhana J.*, **25**(4), 353-365.

Lee, S.W. and Wong, S.C. (1982), "Mixed formulation finite elements for Mindlin theory plate bending", *Int. J. Numer. Meth. Eng.*, **18**, 1297-1311.

Liu, J., Riggs, H.R. and Tessler, A. (2000), "A four node shear-deformable shell element developed via explicit Kirchhoff constraints", *Int. J. Numer. Meth. Eng.,* **49**, 1065-1086.

Morley, L.S.D. (1963), *Skew plates and structures*, Pergamon press, Oxford.

Nagabhushanam, J. and Patnaik, S.N. (1990), "General purpose program to generate compatibility matrix for the integrated force method", *AIAA J.*, **28**, 1838-1842.

Nagabhushanam, J. and Srinivas, J. (1991), "Automatic generation of sparse and banded compatibility matrix for the Integrated Force Method", *Comput. Mech. '91, Int. Conference on Comput. Eng. Scei.,* Patras, Greece.

NISA *Software and manual* (Version 9.3)

Ozgan, K. and Daloglu, A.T. (2007), "Alternate plate finite elements for the analysis of thick plates on elastic foundations", *Struct. Eng. Mech.*, **26**(1), 69-86.

Patnaik, S.N. (1973), "An integrated force method for discrete analysis", *Int. J. Numer. Meth. Eng.*, **41**, 237-251.

Patnaik, S.N. (1986), "The variational energy formulation for the Integrated Force Method", *AIAA J.*, **24**,129-137.

Patnaik, S.N., Berke, L. and Gallagher, R.H. (1991), "Integrated force method verses displacement method for finite element analysis", *Comput. Struct.,* **38**(4), 377-407.

Patnaik, S.N., Coroneos, R.M. and Hopkins, D.A. (2000), "Compatibility conditions of structural mechanics", *Int. J. Numer. Meth. Eng.*, **47**, 685-704.

Patnaik, S.N. Hopkins, D.A. and Coroneos, R. (1986), "Structural Optimization with approximate sensitivities", *Comput. Struct.*, **58**, 407-418.

Patnaik, S.N. and Yadagiri, S. (1976), "Frequency analysis of structures by Integrated Force Method", *Comput. Meth. Appli. Mech. Eng.*, **9**, 245-265.

Pian, T.H.H. (1964), "Derivation of element stiffness matrices by assumed stress distributions", *A.I.A.A J.*, **2**, 1333-1336.

Pian, T.H.H. and Chen, D.P. (1982), "Alternative ways for formulation of hybrid stress elements", *Int. J. Numer. Meth. Eng.*, **19**, 1741-1752.

Przemieniecki, J.S. (1968), *Theory of Matrix Structural Analysis*, McGraw Hill, New York.

Razzaque, A. (1973), "Program for triangular plate bending element with derivative smoothing", *Int. J. Numer. Meth. Eng.*, **6**, 333-345.

Reissner, E. (1945), "The effect of transverse shear deformation on bending of plates", *J. Appl. Mech.*, **12**, A69-A77.

Robinson, J. (1973), *Integrated Theory of Finite Elements Methods*, Wiley, New York

Spilker, R.L. (1982), "Invariant 8-node hybrid-stress elements for thin and moderately thick plates", *Int. J. Numer. Meth. Eng.*, **18**, 1153-1178.

Kim, S.H. and Choi, C.K. (2005), "Modeling of Plates and Shells: Improvement of quadratic finite element for Mindlin plate bending", *Int. J. Numer. Meth. Eng.,* **34**(1), 197-208.

Timoshenko, S.P. and Krieger, S.W. (1959), *Theory of plates and shells*, Second Edition, McGraw Hill International Editions.

Tong, P. (1970), "New displacement hybrid finite element models for solid continua", *Int. J. Numer. Meth. Eng.*, **2**, 73-83.

Notations

$[A]$	= matrix relating nodal degrees of freedom and coefficients of the polynomial
$[B]$	= global equilibrium matrix ($m \times n$)
$[B_e]$	= element equilibrium matrix ($m_e \times n_e$)
$[C]$	= compatibility matrix ($r \times n$)
D	= flexural rigidity of the plate
$[D_{op}]$	= differential operator matrix
E	= Young's modulus
$\{F\}$	= vector of internal forces of the structure ($n \times 1$)
$\{F_e\}$	= vector of internal forces of the discrete element ($n_e \times 1$)
$[G]$	= global flexibility matrix ($n \times n$)
$[G_e]$	= element flexibility matrix ($n_e \times n_e$)
$[H]$	= matrix relating the curvatures to stress resultants
$[J]$	= deformation coefficient matrix ($m \times n$)
L, B	= length and breadth of the plate
M_c	= central moment of the plate
$\{M\}$	= vector of stress resultants
P	= point load at the center or tip of the plate
$\{P\}$	= vector of external loads ($m \times 1$)
q	= uniform load over the plate
$[S]$	= IFM governing matrix ($n \times n$)
W_c	= Central deflection of the plate
$\{X\}$	= vector of displacements of the structure ($m \times 1$)
$\{X_e\}$	= vector of displacements of the discrete element ($m_e \times 1$)
$\{k\}$	= vector of curvatures
n, m	= force and displacement degrees of freedom of the structures respectively
n_e, m_e	= element force and displacement degrees of freedom respectively
t	= thickness of the plate
$\{\alpha\}$	= generalized coordinates of the polynomial in the displacement field.
$\{\beta\}$	= vector of elastic deformations
$\{\beta_o\}$	= vector of initial deformations
ν	= Poisson's ratio
$[\phi_1]$	= matrix of polynomial terms for displacement fields
$[\psi]$	= matrix of polynomial terms for stress-resultants fields

Appendix A: Basic Theory of IFM

In the Integrated Force Method of analysis, a structure idealized by finite elements is designated as "structure (n, m)", where n and m are force and displacement degrees of freedom of the discreet model, respectively. The 'structure (n, m)' has m equilibrium equations (EE) and $r = (n\text{-}m)$ compatibility conditions (CC).

The equilibrium equation (EE) represents the vectorial summation of the internal forces $\{F\}$ to the external loads $\{P\}$ at the nodes of the finite element discretization. It can be written in symbolized matrix notation as:

Equilibrium Eqs. (EE)

$$[B]\{F\} = \{P\} \tag{A.1}$$

where

$[B]$ = global equilibrium matrix $(m \times n)$
$\{F\}$ = vector of internal forces of the structure $(n \times 1)$
$\{P\}$ = vector of external loads on the structure $(m \times 1)$

The compatibility conditions (CC) are constraints on strains, and for finite element models they are also constraints on member deformations.

In IFM St. Venant's approach has been extended for discrete mechanics to develop the compatibility conditions. Development of CC is briefly explained below:

The Deformation-Displacement Relationship (DDR) for discrete mechanics is equivalent to the strain-displacement relationship in elasticity. The DDR for discrete analysis was obtained during the development of the variational energy formulation for the IFM.

According to work energy-conservation theorem, the internal energy (IE) stored in the structure is equal to the work done by the external load (WD), that is

$$I\,E = W\,D$$

$$\frac{1}{2}\{F\}^T\{\beta\} = \frac{1}{2}\{P\}^T\{X\} \tag{A.2}$$

where $\{X\}$ represents nodal displacements. Eq. (A.2) can be rewritten by eliminating the load $\{P\}$ in favor of forces $\{F\}$, by using Eq. (A.1) to obtain the following relation

$$\frac{1}{2}\{F\}^T[B]^T\{X\} = \frac{1}{2}\{F\}^T\{\beta\} \tag{A.3}$$

Eq. (A.3) can be simplified as

$$\frac{1}{2}\{F\}^T[[B]^T\{X\} - \{\beta\}] = 0 \tag{A.4}$$

Because the n forces can be arbitrary and $\{F\}$ is not a null vector, its coefficient should be zero, which yields the DDR as

$$\{\beta\} = [B]^T\{X\} \tag{A.5}$$

where $\{\beta\}$ are member deformations.

This equation represents the Deformation-Displacement Relations (DDR) for the discrete structure. The elimination of m displacements from n deformations displacement relations given by the above equation yields $r = (n - m)$ compatibility conditions and the associated matrix $[C]$. It can be symbolized in matrix notations as

$$[C]\{\beta\} = 0 \tag{A.6}$$

where $[C]$ is the $(r \times n)$ compatibility matrix. It is a kinematic relationship, and is independent of design parameters, material properties and external loads. This matrix is rectangular and banded. The deformation

$\{\beta\}$ in the compatibility conditions (CC) given by the Eq. (A.6) represents the total deformation consisting of an elastic component $\{\beta_e\}$ and the initial component $\{\beta_o\}$ as

$$\{\beta\} = \{\beta_e\} + \{\beta_o\} \tag{A.7}$$

The *CC* in terms of elastic deformation can be written as

$$[C]\{\beta\} = [C]\{\beta_e\} + [C]\{\beta_o\} \tag{A.8}$$

$$[C]\{\beta_e\} = \{\delta R\}$$

where

$$\{\delta R\} = -[C]\{\beta_o\} \tag{A.9}$$

Using element flexibility characteristics, Eq. (A.6) with initial deformation can be rewritten as

$$[C][G]\{F\} = \{\delta R\} \tag{A.10}$$

Clubbing of Eq. (A.1) and Eq. (A.10) will lead to the IFM governing equation as

$$\begin{bmatrix} [B] \\ [C][G] \end{bmatrix} \{F\} = \begin{Bmatrix} P \\ \delta R \end{Bmatrix}$$

$$[S]\{F\} = \{P^*\} \tag{A.11}$$

The solution of the Eq. (A.11) yields *n* forces $\{F\}$. The *m* displacements $\{X\}$ are obtained from the forces $\{F\}$ by back substitution as

$$\{X\} = [J]\{[G]\{F\} + \{\beta_o\}\} \tag{A.12}$$

where $[J] = m$ rows of $[[S]^{-1}]^T$.

Appendix B: The exact solutions for central deflection and bending moment of square plates

The exact solutions for central deflection and bending moment of square plates are given in the Table B1.

Table B1 The exact solutions for central deflection and bending moment of plates

Boundary conditions and loading	W_{thin}	W_{mind}	$M_{thin/mind}$
Simply supported with central point load	$0.011603PL^2/D$	--------	--------
Clamped with central point load	$0.005595PL^2/D$	--------	--------
Simply supported with uniform load	$0.004066qL^4/D$	$0.004270\ qL^4/D$	$0.0479\ qL^2$
Clamped with uniform load	$0.001264PL^4/D$	$0.001500\ qL^4/D$	$0.0231\ qL^2$